Designing a multi-reflection time-of-flight mass analyzer for LPT

Y.L. Tian[a,b], Y.S. Wang[a], J.Y. Wang[a], X.H. Zhou[a], W.X. Huang[a,*]

[a] *Institute of Modern Physics, Chinese Academy of Sciences, Lanzhou 730000, China*
[b] *University of Chinese Academy of Sciences, Beijing 100049, China*

Abstract

A new method including two sub-procedures, global search and local refine, has been developed and presented to design a multiple-reflection time-of-flight (MRTOF) mass analyzer. By using this method, a different type of MRTOF mass analyzer, in which each mirror consists of five cylindrical electrodes, has been designed for isobaric separation for Lanzhou Penning Trap (LPT). The optimal potential parameters of the electrodes have been obtained and the maximal resolving power has been achieved to be 1.3×10^5 with a total time-of-flight of 6.5 ms for an ion species of $^{40}Ar^{1+}$. The simulation shows the inaccuracy of the potentials applied to the mirror electrodes must be less than 50 ppm or preferably 20 ppm.

Keywords: Time-of-flight mass spectrometer, Multiple-reflection, Mass measurement, Isobar separation, Exotic nuclei

1. Introduction

The multi-reflection time-of-flight mass spectrometer (MRTOF-MS) was first proposed by Wollnik [1] more than 25 years ago. It is a device developed in recent years for mass spectrometry and isobar separation with ion bunches with kinetic energies in the range of a few hundreds of electron-volts to a few kilo-electron-volts. By extending the flight path using multi-reflection between electrostatic ion mirrors, the MRTOF-MS overcomes the limitation in resolving power in a conventional time-of-flight mass spectrometer (TOF-MS) and keeps its unique advantages, extremely short measurement time, a large mass range, very high sensitivity and non-scanning operation. It meets the challenges of mass spectrometry at current and future accelerator facilities for the research with exotic nuclei, and it is suitable for experimental measurements for very exotic nuclei with very low production yields and purities and very short half-lives to study their properties.

Plaß et al. [2] reviewed the MRTOF-MS developments for the research with short-lived nuclei and different instrumental implementations. According to the potential along the optical axis, the existing analyzers can be cataloged into two types: asymmetric and symmetric. The asymmetric type was implemented at Oak Ridge National Lab. [3] and RIKEN [4], while the symmetric one was chosen by many researchers in other places around the world. The configuration in Ref. [5], in which each mirror was made of eight cylindrical electrodes, was derived and used for the ISOLTRAP experiments [6] at ISOLDE/CERN and made great achievements for mass measurements [7, 8] and isobaric separations. A duplicate of this maybe will be operated at RAON/RISP [9]. An advanced coaxial four-electrode design has been implemented for the LEB of the Super-FRS at FAIR [10], for TITAN [11], and for MLL-TRAP [12]. As we know, MRTOF-MS is also being implemented in ANL [13] and IGISOL [14].

The Lanzhou Penning Trap (LPT) [15] is an ion trap facility that is presently under construction at the Institute of Modern Physics, Chinese Academy of Sciences. We also plan to build an MRTOF-MS for isobaric separation for the LPT. Since the number of electrodes affects the potential smoothing along the optical axis and determines the number of power supplies, thus the cost of whole device, we try to design a new type of MRTOF mass analyzer with a different configuration, in which each mirror consists of five cylindrical electrodes.

In this paper we concentrate only on the design and optimization of our MRTOF mass analyzer and the corresponding results. The injection and ejection of the ions into and out of the analyzer are ignored.

2. Design of the MRTOF mass Analyzer

The being-designed MRTOF mass analyzer shown in Fig. 1 consists of two identical electrostatic mirrors (each a set of four electrodes) in combination with two einzel lenses and a drift-tube. The ions coming from an upstream RFQ cooler/buncher enter into the analyzer by switching down the potentials on the mirror electrodes. Afterwards the mirror-electrode potentials are activated again and the ions travel hundreds of revolutions between the two mirrors and are separated by their mass-to-charge ratio during the oscillations inside the device. The ions of interest are released from the analyzer by switching down the mirror-electrode potentials and then arrive at a time focus plane, where an MCP detector for mass measurements or a Bradbury-Nielsen gate [16] for isobaric separation is deployed.

*Corresponding author
Email addresses: yltianok@impcas.ac.cn (Y.L. Tian), huangwx@impcas.ac.cn (W.X. Huang)

All electrodes of this analyzer have a cylindrical shape. The total length is 708 mm with an inner diameter of 60 mm. The mirror electrodes M1-M4 have lengths of 20, 16, 26, and 26 mm, respectively, and the lens electrode L has 46 mm. The electrode M1 has a smaller aperture of 30 mm diameter at the outer end for electric shielding of the analyzer from the adjacent parts. The intermediate drift-tube has a length of 400 mm (optimized later) and two reduced apertures of 30 mm diameter at each end to shield the drift region from electric fields of the lens electrode. The distance between two adjacent electrodes is 4 mm. The time focus plane where an MCP detector or a Bradbury-Nielsen gate can be placed, are located 255 mm after the analyzer.

The mass resolving power R is defined as mass m divided by the difference of neighboring masses that can still be distinguished Δm and related to the time-of-flight TOF and the temporal width ΔTOF by $R = m/\Delta m = TOF/2/\Delta TOF$, where the overall spread ΔTOF is the full-width-at-half-maximum (FWHM) of the time-of-flight peak. The ΔTOF value depends not only on the initial bunch width of the ion bunch, but also on the time-of-flight aberration from the start point to the time focus plane.

3. Optimization procedure

To find the optimal parameters with the structure shown in Fig. 1, an optimization strategy has to be performed. Ref. [17] has provided a procedure for the potential parameter optimization, in which a Nelder-Mead simplex algorithm [18] is used in the code SIMION [19] and the ion trajectory meeting the point-to-parallel/parallel-to-point focusing condition for highest trajectory stability has to be found first. We think it is possible that the optimal parameter sets may not be found using this optimization procedure. The point-to-parallel/parallel-to-point focusing condition is very easy to satisfy, and a lot of parameter sets which ion trajectories meet this focusing condition can be found for the mass analyzer even in a very small parameter space. It is time-consuming to find more in a larger space and it is difficult to know whether the best start point has already been found in a limited time. So we employ another procedure, which includes two sub-procedures, a global search and a local refine. In our procedure, ion trajectories were calculated in the SIMION according to our specified user program as usual, and the variation of the parameters by the Nelder-Mead simplex algorithm was performed in a separate optimization program that is coded by ourselves. The advantages for this procedure are (1) the best parameters can be found for sure, because we search all the possibilities in the whole parameter space; (2) the optimization program does not need to be changed if the structure of the MRTOF mass analyzer is varied. By this procedure we can find the optimal parameters for not only the analyzer, but also the whole MRTOF-MS including more elements, such as einzel lens for the injection and ejection of the beam.

The details of the procedure are given in the following. At first, a model is created in the SIMION according to the configuration of the MRTOF-MS, in which the average and the deviation of the TOF and the resolving power can be calculated. Secondly, for the global search, the possible potential for every electrode is estimated roughly according to the knowledge of the beam optics and the variation from the possible potential is set deliberately, thus a potential matrix with several dimensions, which equals to the parameters to be optimized, will be created as the initial parameter sets for the search. Then, all the initial parameter sets will be input into the SIMION and the ion trajectories will be calculated for the same species, and a few sets with relatively high resolving power for a specified number of revolutions inside the analyzer are chosen out. Thirdly, for the local refine, all parameters are varied by the Nelder-Mead simplex algorithm in these parameter sets and input into the SIMION again and the peak width of the same species is measured and treated as the goal function to be minimized. After approaching a local minimum of the TOF surface within a certain radius, these optimized parameters where multiplied by random numbers close to 1 and the optimization is restarted. With this procedure, a large number of local minima can be obtained and the best are chosen to be the optimal parameter sets.

4. Results and discussion

To calculate the mass resolving power with respect to the number of revolutions, we considered the following as initial beam conditions. The beam consists of 100 ions (if not specified) of $^{40}Ar^{1+}$, of which the average kinetic energy is 1.5 keV, and the bunch width is 20 ns (FWHM) at the middle of the analyzer. In the middle between the ion mirrors the ion beam coordinates x and y orthogonal to the optical axis z, the angles α=dx/dz and β=dy/dz with respect to the axis z and the energy K are approximately represented by Gaussian distributions with standard deviations σ_x=σ_y=1 mm, σ_α=σ_β=1.5 mrad and σ_K=8.5 eV.

4.1. Optimization of potential distribution and the length of drift-tube

Considering the symmetric shape of the being-designed MRTOF analyzer and the practical potential control through the power supplies during the experiments, we set the potentials applied on the four mirror electrodes and one lens electrode as the optimization parameters, five in total. The potential on the inner drift-tube was fixed to 0 during all the calculations.

In the global search step, we considered 6×6×5×6×6=6480 potential combinations in total as the initial parameter sets and at last chose only the best five sets for further local refine. By the Nelder-Mead simplex algorithm all parameters were varied and a large number of local minima were obtained. We chose the parameter set which gives the smallest peak width of the TOF as the optimal one.

In order to achieve a very high resolving power, we also tried to optimize the length of the drift-tube by fixing all the other parameters, thus optimizing the flight times that the ion travels in the drift-tube and in the mirrors. Fig. 2 shows the calculated mass resolving power as function of the length of drift tube. The highest resolving power can be reached when the drift-tube has a length of 398–402 mm and we chose the length of 400 mm as our optimal result.

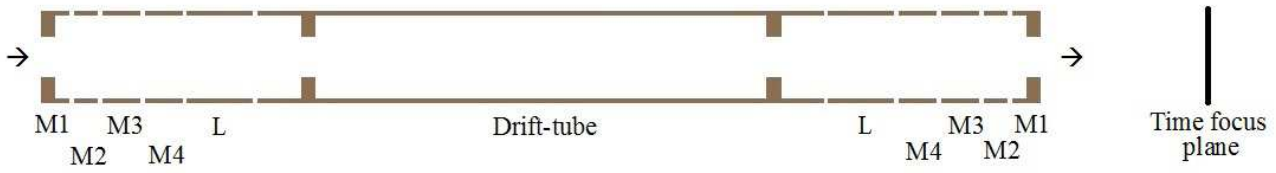

Figure 1: The geometry of the being-designed MRTOF mass analyzer. The time focus plane (detector plane) is also shown.

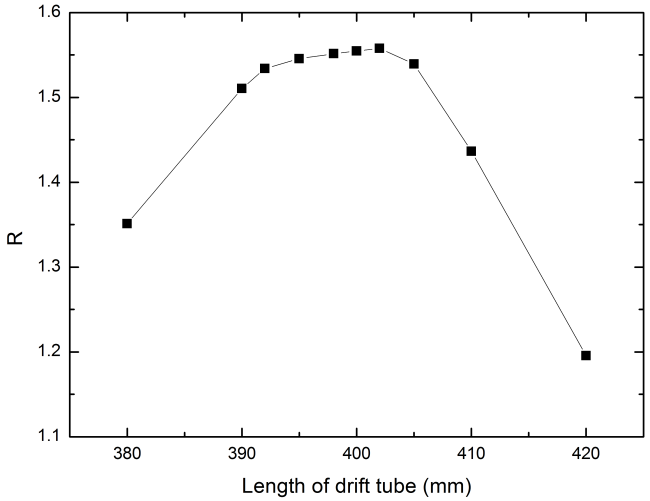

Figure 2: Calculated mass resolving power R as function of the length of drift tube

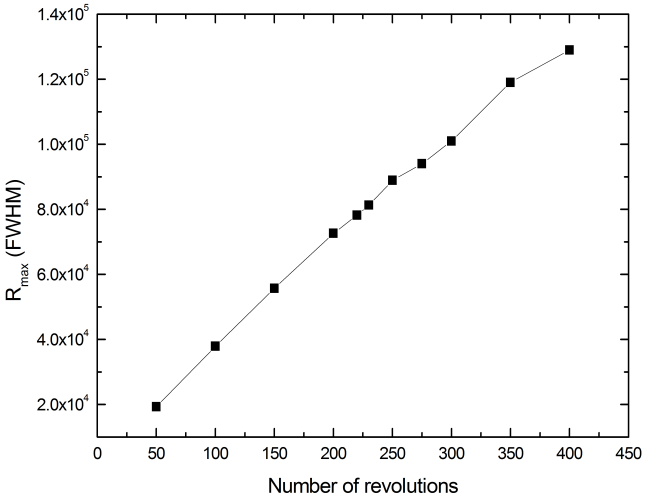

Figure 3: The maximal mass resolving power R_{max} achieved at different number of revolutions

Table 1: Optimized potentials on the mirror-electrodes and the lens electrode shown in Fig. 1 for the $^{40}Ar^{1+}$ ions. M1 – M4: mirror electrodes 1 – 4 from outside to inside, L: lens electrode.

Electrode	M1	M2	M3	M4	L
Potential (V)	2502.5	2002.2	1420.9	817.1	−4473.1

By fixing the length of the drift-tube at 400 mm we optimized the potentials for different number of revolutions and obtained the maximal resolving power that can be achieved, shown in Fig. 3. As increasing the number of revolutions up to 400 the maximal resolving power increases steadily but the slope of this increase drops. This may mean that if we attempt to achieve a higher mass resolving power we should let the ions fly a longer distance in the MRTOF analyzer. Since the calculation is very time-consuming we did not continue the optimization for a larger number of revolutions more than 400.

For every optimization for a specific number of revolutions we have obtained one potential set with the highest mass resolving power. Table 1 lists the potentials optimized for the number of revolutions of 350. Fig. 4 shows the distribution of the potential along the optical axis in one of the mirrors of the analyzer. It has two regions with approximately constant electric fields [20, 21], $E_1 < E_2$. The ions turn around in the weaker constant electric field E_1.

Applying the potentials in Table 1 to the electrodes, we have calculated the temporal width at the detector plane with respect to the number of revolutions. Fig. 5 shows the calculation re-

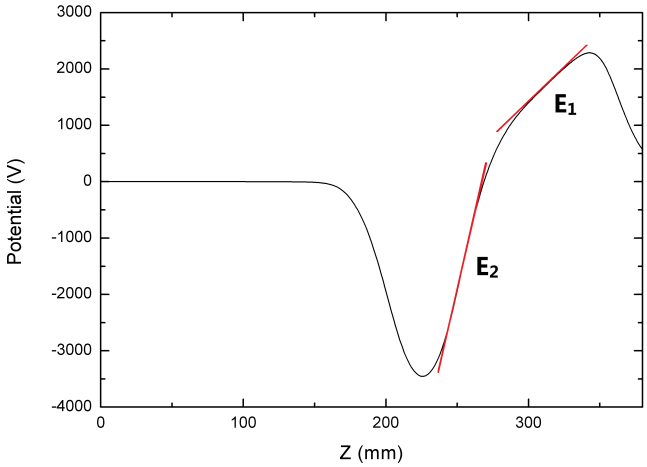

Figure 4: Potential distribution at the optical axis z in one of the mirrors of the MRTOF analyzer for the mean ion kinetic energy of 1.5 keV. The position $z = 0$ corresponds to the middle point between the ion mirrors. E_1 and E_2 are two regions with approximately constant electric fields.

sults of the total TOF, the temporal width ΔTOF, and the mass resolving power R as function of number of revolutions. Increasing the number of revolutions, the total time-of-flight almost increases linearly, and the initially high temporal spread decreases until a minimum, only 22 ns at the number of revolutions of 350, where the resolving power reaches 1.1×10^5. The maximal resolving power R=1.3×10^5 is achieved at 430 laps (TOF=6.5 ms), since the temporal spread increases slower than the total time-of-flight of the ions in the MRTOF analyzer.

4.2. Effects of potential inaccuracy

Fig. 6 shows the relative variation of TOF and mass resolving power as functions of the relative variation of the bias potentials as determined by our optimization code. For the TOF, the behavior from the mirror electrode M4 acts differently from other electrodes, and the largest variation is from the mirror electrode M2. The maximal achievable mass resolving power decreases as the potentials applied on the electrodes vary from the ideal ones as expected. The potential variations of the mirror electrode M4 and the lens electrode L, for which form an einzel lens with the drift tube, almost have no effect on the final resolving power; those from the mirror electrodes M1 and M2 have relative bigger effect; and that from the mirror electrode M3 has the biggest effect, which the resolving power decreases 35% from 1.1×10^5 to 7.0×10^4 as the relative variation of the potential by 500 ppm. Thus we have to assure that the potentials applied to the mirror electrodes M1–M3, especially M3 are stable to less than 50 ppm or preferably 20 ppm.

4.3. Peak shape

In order to accurately determine the TOF and understand the peak shape, we extracted the TOF spectra shown in Fig. 7. In the calculation the potentials listed in Table 1 were applied to the electrodes and the beam properties kept the same mentioned before except 2500 ions were used instead for increasing statistics. Apparently the peak shape can be fitted by a Gaussian function with a FWHM of 21.6 ns. This does not agree with the result reported in Ref. [22], where the authors showed that the TOF peak was fitted by an exponential-Gaussian hybrid than a Gaussian function and stated that the slow-side tail maybe related to higher-order optical aberrations.

5. Summary

A new method to design a multiple-reflection time-of-flight mass analyzer is presented. It includes two sub-procedures, global search and local refine. This method has the following advantages: (1) the best parameters can be found for sure; (2) the optimization program does not need to change if the structure of the MRTOF analyzer is varied. It also has the capability to find the optimal potentials related to the whole MRTOF mass spectrometer or isobar separator.

By using this new method, an MRTOF mass analyzer, in which each mirror consists of five cylindrical electrodes, has been designed. The optimal potential parameters of the electrodes have been obtained and the maximal resolving power has been achieved to be 1.3×10^5 with a total TOF of 6.5 ms for an ion species of $^{40}Ar^{1+}$. The simulation shows the potentials applied to the mirror electrodes M1–M3, especially M3 must have an inaccuracy of less than 50 ppm or preferably 20 ppm. This analyzer together with the injection and ejection elements will be mounted to the beamline of the LPT for isobar separation.

Acknowledgments

This work was supported by the National Natural Science Foundation of China (Grant Nos: 11405243, 11075188), the Chinese Academy of Sciences (No. 113462KYS820150026), and the National Basic Research Program of China (973 Program) (No. 2013CB834400).

[1] H. Wollnik, M. Przewloka, Time-of-flight mass spectrometers with multiply reflected ion trajectories, International Journal of Mass Spectrometry and Ion Processes 96 (1990) 267-274.

[2] W.R. Plaß, T. Dickel, C. Scheidenberger, Multiple-reflection time-of-flight mass spectrometry, International Journal of Mass Spectrometry 349-350 (2013) 134-144.

[3] A. Piechaczek, V. Shchepunov, H.K. Carter, J.C. Batchelder, E.F. Zganjar, S.N. Lid-dick, H. Wollnik, Y. Hu, B.O. Griffith, Development of a high resolution isobar separator for study of exotic decays, Nuclear Instruments and Methods in Physics Research Section B 266 (2008) 4510-4514.

[4] P. Schury, K. Okada, S. Shchepunov, T. Sonoda, A. Takamine, M. Wada, H.Wollnik, Y. Yamazaki, Multi-reflection time-of-flight mass spectrograph for short-lived radioactive ions, European Physical Journal A 42 (2009) 343-349

[5] H.B. Pedersen, D. Strasser, S. Ring, O. Heber, M.L. Rappaport, Y. Rudich, I. Sagi, D. Zajfman, Ion Motion Synchronization in an Ion-Trap Resonator, Physical Review Letters 87 (2001) 055001.

[6] R.N. Wolf, F. Wienholtz, D. Atanasov, D. Beck, K. Blaum, Ch. Borgmann, F. Herfurth, M. Kowalska, S. Kreim, Yu.A. Litvinov, D. Lunney, V. Manea, D. Neidherr, M. Rosenbusch, L. Schweikhard, J. Stanja, K. Zuber, ISOLTRAP's multi-reflection time-of-flight mass separator/spectrometer, International Journal of Mass Spectrometry 349-350 (2013) 123-133.

[7] R.N. Wolf, D. Beck, K. Blaum, Ch.Böhm, C. Borgmann, M. Breitenfeldt, N. Chamel, S. Goriely, F. Herfurth, M. Kowalska, S. Kreim, D. Lunney, V. Manea, E.M. Ramirez,S. Naimi, D. Neidherr, M. Rosenbusch, L. Schweikhard, J. Stanja, F. Wienholtz, K. Zuber, Plumbing neutron stars to new depth with the binding energy of the exotic nuclide ^{82}Zn, Physical Review Letters 110 (2013) 041101.

[8] F. Wienholtz, D. Beck, K. Blaum, C. Borgmann, M. Breitenfeldt, R.B. Cakirli, S. George, F. Herfurth, J.D. Holt, M. Kowalska, S. Kreim, D. Lunney, V. Manea, J. Menendez, D. Neidherr, M. Rosenbusch, L. Schweikhard, A. Schwenk, J. Simonis, J. Stanja, R.N. Wolf, K. Zuber, Masses of exotic calcium isotopes pin down nuclear forces, Nature 498 (2013) 346-349.

[9] J.W. Yoon, Y.-H. Park, S.J. Park, G.D. Kim, Y.K. Kim, Design of the multi-reflection time-of-flight mass spectrometer for the RAON facility, EPJ Web of Conferences 66 (2014) 11042.

[10] W.R. Plaß, T. Dickel, U. Czok, H. Geissel, M. Petrick, K. Reinheimer, C. Scheidenberger, M.I. Yavor, Isobar separation by time-of-flight mass spectrometry for low-energy radioactive ion beam facilities, Nuclear Instruments and Methods in Physics Research Section B 266 (2008) 4560-4564.

[11] T. Dickel, C. Jesch, W.R. Plaß, S. Ayet, U. Czok, H. Geissel, F. Lautenschläger, M. Petrick, C. Scheidenberger, B. Sun, M.I. Yavor, Further advances in the devel-opment of a multiple-reflection time-of-flight mass spectrometer for isobarseparation and massmeasurements at the LEB, GSI Scientific Report 2010 (2011) 139.

[12] C. Weber, P. Müller, P.G. Thirolf, Developments in Penning trap (mass) spectrometry at MLLTRAP: Towards in-trap decay spectroscopy, International Journal of Mass Spectrometry 349-350 (2013) 270-276.

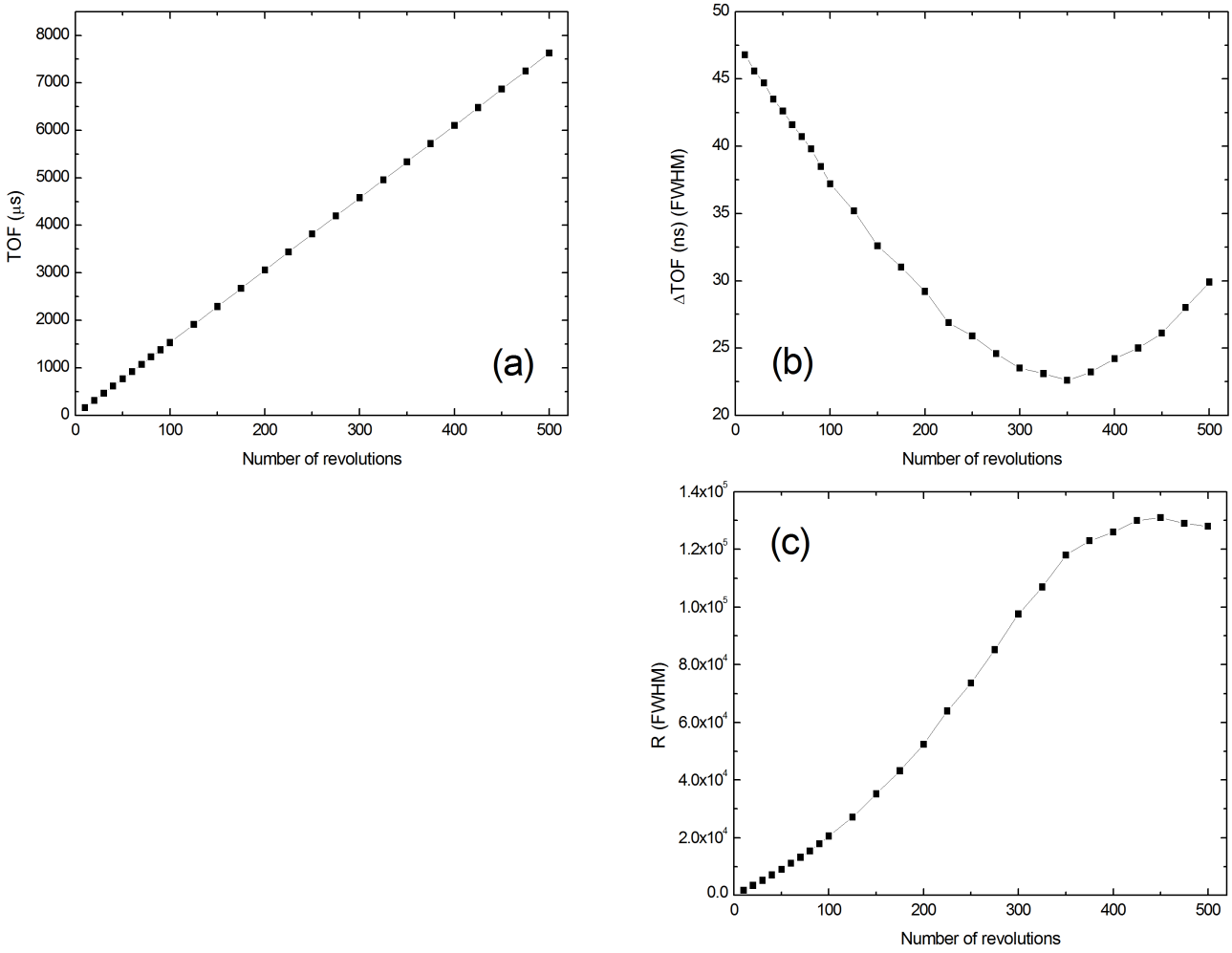

Figure 5: Calculation results of the TOF (a), the temporal width ΔTOF (b), and the mass resolving power R (c) as function of number of revolutions.

[13] J. Van Schelt, D. Lascar, G. Savard, J.A. Clark, P.F. Bertone, S. Caldwell, A. Chaudhuri, A.F. Levand, G. Li, G.E. Morgan, R. Orford, R.E. Segel, K.S. Sharma, M.G. Sternberg, First Results from the CARIBU Facility: Mass Measurements on the r-Process Path, Physical Review Letters 111 (2013) 061102.

[14] I.D. Moore, T. Eronen, D. Gorelov, J. Hakala, A. Jokinen, A. Kankainen, V.S. Kolhinen, J. Koponen, H. Penttilä, I. Pohjalainen, M. Reponen, J. Rissanen, A. Saastamoinen, S. Rinta-Antila, V. Sonnenschein, J. Äystö, Towards commissioning the new IGISOL-4 facility, Nuclear Instruments and Methods in Physics Research Section B: Beam Interactions with Materials and Atoms 317, Part B (2013) 208-213.

[15] W.X. Huang, Y.L. Tian, J.Y. Wang, Y.L. Sun, Y.S. Wang, Y. Wang, J.M. Zhao, W. Wu, L.Z. Ma, Y. He, H.S. Xu, G.Q. Xiao, Status of Lanzhou Penning Trap for accurate mass measurements, Nuclear Instruments and Methods in Physics Research Section B: Beam Interactions with Materials and Atoms 317, Part B (2013) 528-531.

[16] N.E. Bradbury, R.A. Nielsen, Absolute values of the electron mobility in hydrogen, Physical Review 49 (1936) 388-393.

[17] R. Wolf, M. Eritt, G. Marx, L. Schweikhard, A multi-reflection time-of-flight mass separator for isobaric purification of radioactive ion beams, Hyperfine Interactions 199 (2011) 115-122.

[18] J. Nelder, R. Mead, Comput. J., Oxford Univ. Press 7 (1965) 308.

[19] D.J. Manura, D.A. Dahl, SIMION 8.0 User Manual, Scientific Instrument Services, Inc., Idaho National Laboratory, 2006.

[20] H. Wollnik, A. Casares, International Journal of Mass Spectrometry 227 (2003) 217-222.

[21] B.A. Mamyrin, V.I. Karataev, D.V. Shmikk, V.A. Zagulin, Sov. Phys. JETP 37 (1973) 45.

[22] P. Schury, M. Wada, Y. Ito, F. Arai, S. Naimi, T. Sonoda, H. Wollnik, V.A. Shchepunov, C. Smorra, C. Yuan, A high-resolution multi-reflection time-of-flight mass spectrograph for precision mass measurements at RIKEN/SLOWRI, Nuclear Instruments and Methods in Physics Research Section B: Beam Interactions with Materials and Atoms 335 (2014) 39-53.

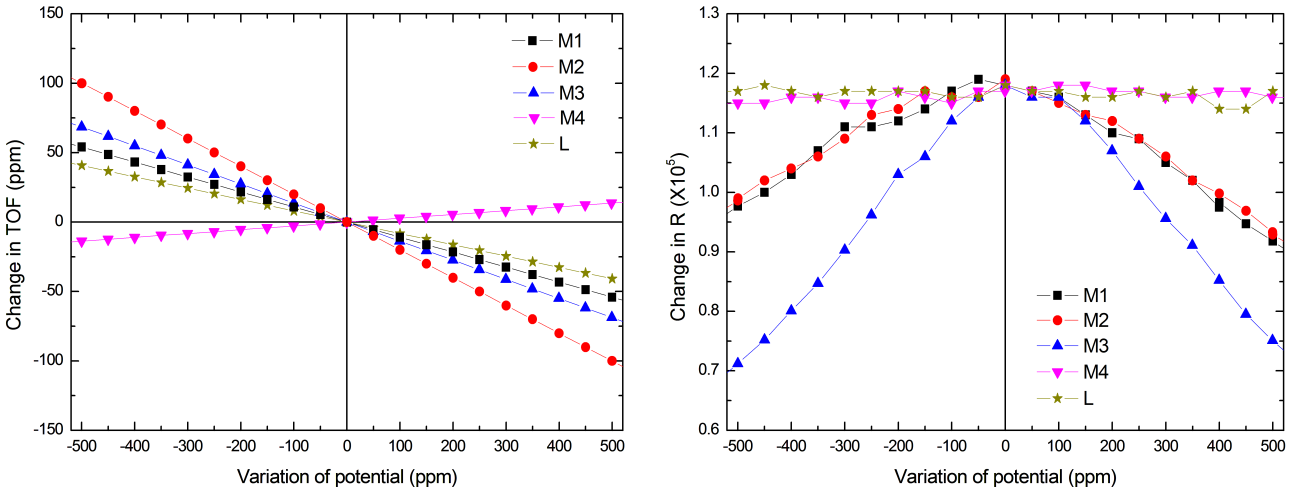

Figure 6: Calculated relative variation of TOF (left) and mass resolving power R (right) as functions of relative variation of bias potentials as determined by optimization code

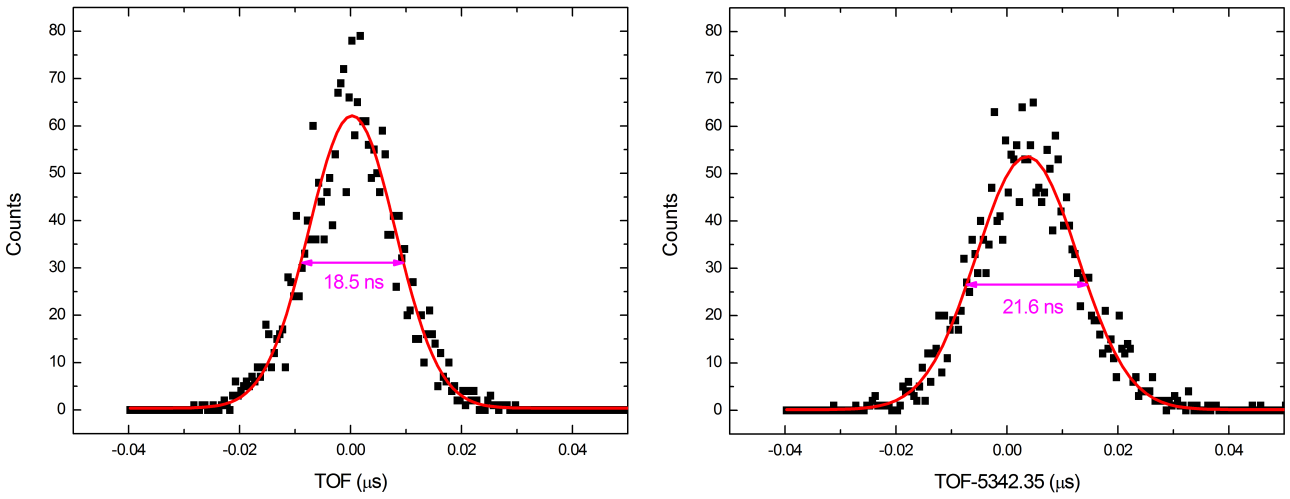

Figure 7: Left: The initial TOF distribution of the ions with $^{40}Ar^{1+}$ (m/q=40). Right: The calculated TOF distribution of the ions after 350 laps in the MRTOF analyzer. The total ion number is 2500. The red lines are fitting results by a Gaussian function.